

This article was downloaded by:

On: 16 January 2011

Access details: *Access Details: Free Access*

Publisher *Taylor & Francis*

Informa Ltd Registered in England and Wales Registered Number: 1072954 Registered office: Mortimer House, 37-41 Mortimer Street, London W1T 3JH, UK



Journal of Energetic Materials

Publication details, including instructions for authors and subscription information:

<http://www.informaworld.com/smpp/title~content=t713770432>

Computational Study of Main Mechanisms for Gas-Phase Decomposition of 1,1- and 1,2-Dinitroethane

Roman V. Tsyshevsky^a; Ilia V. Aristov^a; Denis V. Chachkov^a; Alexander G. Shamov^a; Grigorii M. Khrapkovskii^a

^a Department of Computational Chemistry, Kazan State Technological University, Russian Federation, Kazan

Online publication date: 15 October 2010

To cite this Article Tsyshevsky, Roman V. , Aristov, Ilia V. , Chachkov, Denis V. , Shamov, Alexander G. and Khrapkovskii, Grigorii M.(2010) 'Computational Study of Main Mechanisms for Gas-Phase Decomposition of 1,1- and 1,2-Dinitroethane', *Journal of Energetic Materials*, 28: 4, 318 – 337

To link to this Article: DOI: 10.1080/07370651003800932

URL: <http://dx.doi.org/10.1080/07370651003800932>

PLEASE SCROLL DOWN FOR ARTICLE

Full terms and conditions of use: <http://www.informaworld.com/terms-and-conditions-of-access.pdf>

This article may be used for research, teaching and private study purposes. Any substantial or systematic reproduction, re-distribution, re-selling, loan or sub-licensing, systematic supply or distribution in any form to anyone is expressly forbidden.

The publisher does not give any warranty express or implied or make any representation that the contents will be complete or accurate or up to date. The accuracy of any instructions, formulae and drug doses should be independently verified with primary sources. The publisher shall not be liable for any loss, actions, claims, proceedings, demand or costs or damages whatsoever or howsoever caused arising directly or indirectly in connection with or arising out of the use of this material.

Computational Study of Main Mechanisms for Gas-Phase Decomposition of 1,1- and 1,2-Dinitroethane

ROMAN V. TSY SHEVSKY, ILIA
V. ARISTOV, DENIS V. CHACHKOV,
ALEXANDER G. SHAMOV,
and GRIGORII M. KHRAPKOVSKII

Department of Computational Chemistry, Kazan State
Technological University, Russian Federation, Kazan

The gas-phase enthalpies of formation of 1,1- and 1,2-dinitroethane and corresponding radical products were calculated using G3B3, CBS-QB3 composite methods and DFT B3LYP level of theory with various basis sets. The enthalpies of the C–N, C–C bonds dissociation and activation enthalpies for HONO elimination were also calculated and compared with available experimental data. It was found that G3B3 calculations do provide a reasonable way to tackle the problem of the decomposition channels of 1,1- and 1,2-dinitroethane. Four main mechanisms for gas-phase decomposition of 1,1- and 1,2-dinitroethane were studied using G3B3 model chemistry. HONO elimination seems to be the most favorable mechanism for the decomposition of 1,2-dinitroethane. However, the difference in energies of the HONO elimination and C–N homolytic bond cleavage in 1,1-dinitroethane does not allow to favor any of these

Address correspondence to Roman V. Tsyshesky, Kazan State Technological University, Department of Computational Chemistry, K. Marks, 68, Box 170, Russian Federation, Kazan 420015, Russia. E-mail: roman.tsyshesky@yahoo.com

channels, especially at the working temperature. Gauche conformation of 1,2-dinitroethane is calculated to be the lowest-energy minimum.

Keywords: composite methods, 1,1-dinitroethane, 1,2-dinitroethane, decomposition, DFT

Introduction

Decomposition of nitroalkanes with one or more nitro groups is the subject of a great number of theoretical and experimental explorations [1–4]. Spokes and Benson [1] concluded that the major products of the 1- and 2-nitropropane decomposition were olefins and HONO through a concerted molecular elimination mechanism. The competitive mechanism via C–N homolytic bond fission was studied by Shaw [2]. Wodtke et al. used a modified Rice-Ramsperger-Kassel-Marcus (RRKM) theory to determine the isomerization barrier height for the process of nitro–nitrite rearrangement ($\text{CH}_3\text{NO}_2 \rightarrow \text{CH}_3\text{ONO}$) [3].

In 2003, Denis et al. [5] performed a study of the important decomposition channels on the potential energy surface of nitroethane and 2-nitropropane, employing B3LYP/6-311+G(3df,2p) level of theory. They concluded that in the cases of the enthalpies of formation and potential energy surfaces, the B3LYP/6-311+G(3df,2p)-calculated data seem to agree well with available experimental data. The HONO elimination pathway was calculated to be the most favorable mechanism for the decomposition of nitroethane and 2-nitropropane. The isomerization to aci-form reactions are the most unlikely of the rest possible mechanisms.

Regarding the decomposition channels of dinitroalkanes, Shaw reported the values of activation energies for decomposition reactions of 1,1-dinitroethane (**1**), 1,2-dinitroethane (**2**) through HONO elimination, 47.0 and 46.0 kcal/mol, respectively, and simple C–N bond rupture 49.0 and 62.0 kcal/mol, respectively [2]. Activation energies of C–C and C–N bonds cleavage in **1** reported by Manelis et al. [4] are 91.7 and 47.1 kcal/mol, respectively.

To our knowledge, theoretical study of decomposition of dinitroalkanes employing modern quantum chemical methods analogous to Denis et al. [5] has not been held. Therefore, we decided to make a theoretical study of the potential energy surfaces of **1** and **2**. The comparison of calculated and available experimental data was made with the purpose of determining the most accurate method for further investigation of dinitroalkanes unimolecular decomposition.

Methods

Density functional methods (DFT) [6,7] and modern quantum chemistry composite methods were employed in this study. The B3LYP method, which includes Becke's three-parameter hybrid functional (B3) [8] using the correlation functional of Lee, Yang, and Parr with both local nonlocal terms (LYP) [9,10], was employed with 6-31G(d), 6-311G(2df,p), 6-311++G(df,p), and 6-311++G(3df,3pd) basis sets [11] to hold calculations at DFT level of theory. Composite methods were performed by G3B3 [12] and CBS-QB3 [13,14] model chemistry. All calculations were performed with the program *Gaussian 03* [15]. Structures' states were characterized as true transition states by checking whether they had only one imaginary harmonic vibrational frequency. The intrinsic reaction coordinate (IRC) calculations were held employing B3LYP/6-31G(d) level of theory. Energies of the stationary points were initially calculated at the B3LYP/6-31G(d) level and then further estimated using the G3B3 method. Unrestricted B3LYP is used for the radical decomposition mechanisms. The energies of radical decomposition mechanisms include basis set superposition error (BSSE).

Results and Discussion

The lowest-energy structures of **1** and **2** are depicted in Fig. 1. Tafipolsky et al. [16] and Kiselev and Gritsan [17] have reported that geometrical parameters of nitrosubstituted methanes with one or more nitro groups, computed at the various levels of theory, are very close and in good agreement with experiment.

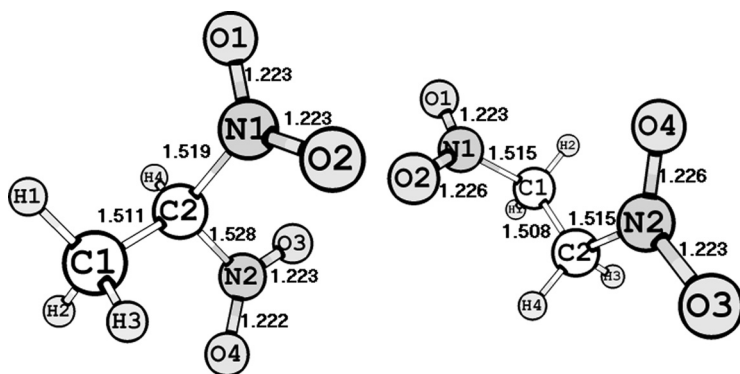


Figure 1. Geometric parameters of the lowest-energy structures of **1** and **2**. Bond distances in Å.

Therefore, in further discussion we will mention the values of geometric parameters obtained only at the B3LYP/6-31G(d) level of theory.

It is worth noting that the lowest energy minimum found on the ground-state potential energy surface (PES) concerning **2** corresponds to the gauche-conformation. The optimized geometry of this global minimum shows the dihedral angle N1C1C2N2 of 71.8 degrees (Fig. 1). Our results agree well with the experimental and calculated data reported by Lam et al. [18]. Their X-ray structure determination showed a central C–C bond distance of 1.488 Å, which is significantly shorter than the standard tetrahedral C–C bond distance (1.544 Å). The molecule as a whole adopted a gauche-conformation with N–C–C–N torsion angle of 73.5 degrees.

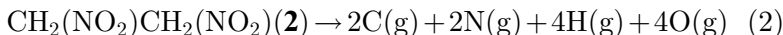
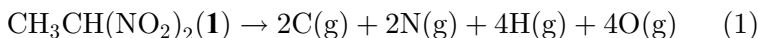
The next stage of our study was determining the proper quantum chemistry methods for further exploration of the mechanisms of decomposition. This procedure was based on comparison of the calculated estimations with available experimental data.

Table 1 shows the gas-phase formation enthalpies of the **1** and **2** predicted at various levels of theory as well as experimental values [19].

Table 1
Enthalpies of formation of **1** and **2**

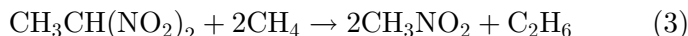
Method	ΔH_{f298}° (kcal/mol)			
	$\text{CH}_3\text{CH}(\text{NO}_2)_2$		$\text{CH}_2\text{NO}_2\text{CH}_2\text{NO}_2$	
	Atomization approach	Isodesmic reaction	Atomization approach	Isodesmic reaction
B3LYP/6-31G(d)	-16.8	-20.7	-21.1	-25.0
B3LYP/6-311G(2df,p)	-22.8	-21.2	-27.1	-25.5
B3LYP/6-311++G(df,p)	-8.7	-46.8	-13.6	-51.7
B3LYP/6-311++G(3df,3pd)	-21.8	-18.4	-26.9	-23.4
CBS-QB3	-26.1	-22.2	-30.3	-26.4
G3B3	-24.2	-23.2	-27.7	-26.7
Experiment [19]	-24.4			-22.9

Enthalpies of formations of **1** and **2** were calculated based on the atomization reactions



An analogous technique was also involved for estimation of enthalpies of formation of the corresponding radicals left after homolytic cleavage of C–N and C–C bonds in **1** and **2** (Table 2).

We also calculated the enthalpies of formation of **1** and **2**, using the isodesmic reaction (3):



The enthalpy of formation of CH_3NO_2 is represented in Lebedev et al. [19], whereas enthalpies of formation of CH_4 and C_2H_6 were taken from the NIST Chemistry Webbook [20].

As one can see from Table 1, enthalpies of formation of **1** predicted using a composite method are in good agreement with experimental values. On the other hand, the enthalpies of formation of **2** calculated at these levels of theory are overestimated. However, results reported in the literature [5,17,21] show that enthalpies of formations of alkanes and nitroalkanes predicted using composite methods are in good agreement with experimental data and do not depend on the size of the molecules. Moreover, repulsion between similarly charged nitro groups attached to same carbon atom ought to increase the enthalpy of formation of **1** in comparison with **2**. For example, experimental enthalpies of formations of 1,1- and 1,3-dinitropropane reported in Lebedev et al. [19] are -28.6 , and -31.6 kcal/mol, respectively. It is worth noting that in accordance with results listed in Table 1, enthalpy of formation of **2** is predicted to be lower than that for **1** at various levels of theory. Therefore, we concluded that experimental enthalpy of formation of **2**, reported in Lebedev et al. [19], is overestimated, whereas the G3B3 calculated value seems to be satisfactory.

Table 2
Enthalpies of formation of the corresponding radicals left after homolytic cleavage of C–N and C–C bonds in **1** and **2**

Method	ΔH_{f298}° (kJ/mol)						
	$\text{CH}_3\text{CH}(\text{NO}_2)\bullet$	$\text{CH}_2\text{NO}_2\text{CH}_2\bullet$	$\text{CH}_3\bullet$	$\bullet\text{CH}(\text{NO}_2)_2$	$\bullet\text{CH}_2\text{NO}_2$	NO_2	NO_2
Experiment [19]	18.2	—	35.0	37.5	—	8.0	8.0
B3LYP/6-31G(d)	17.5	26.6	34.7	38.6	30.3	5.5	5.5
B3LYP/6-311G(2df,p)	14.7	23.5	33.8	31.2	26.6	1.2	1.2
B3LYP/6-311++G(df,p)	21.7	30.3	34.2	44.4	32.1	6.7	6.7
B3LYP/6-311++G(3df,3pd)	13.9	22.7	32.8	32.3	25.4	1.5	1.5
CBS-QB3	17.1	24.8	35.5	36.1	29.3	6.1	6.1
G3B3	18.8	25.4	34.4	38.8	30.9	7.6	7.6

It is worth noting that formation enthalpies of **1** calculated using atomization reactions are more accurate than that calculated via isodesmic reaction.

Unfortunately, the enthalpies of formation of initial compounds and radical products calculated (Table 2) at the B3LYP level of theory with various basis sets are not so accurate. Although B3LYP/6-311G(2df,p) predicts enthalpy of formation of **1** to be only 0.4 kcal/mol lower than experimental value, the calculated enthalpies of formation of radical fragments differ noticeably from experimental data (Table 2).

Denis et al. [5] reported that this method is quite accurate in predictions of enthalpies of formation of nitroethane and 2-nitropropane. B3LYP/6-311+G(3df,2p)-calculated enthalpies of formations of **1** and **2** are in poor agreement with experiment and calculated to be -21.4 and -25.1 kcal/mol, respectively. That is why the data obtained using this method will not be mentioned in our further discussion.

Table 2 demonstrates that composite methods CBS-QB3 and G3B3 predict the enthalpies of formation of radical products with accuracy better than 2 kcal/mol.

The calculated enthalpies of the C-N and C-C bonds dissociation at 298 K as well as related experimental data are listed in Table 3.

The radical mechanism of the nitroalkane decomposition is one of the most investigated processes [2,4]. Dissociation enthalpy of the R₁-R₂ bond in nitrocompounds can be calculated according to Eq. (4):

$$\Delta H^0(R_1 - R_2) = \Delta H_f^0(R_1) + \Delta H_f^0(R_2) - \Delta H_f^0(R_1 - R_2) \quad (4)$$

where R₁ and R₂ are radicals left after the bond decomposition. Dissociation enthalpies of the C-C and C-N bonds estimated according to Eq. (5) are applicable in various calculations and experimental (thermochemical) estimations.

When comparing calculated and experimental data for the radical mechanism the following relation should be hold:

$$E_a = \Delta H^0(R_1 - R_2) + RT \quad (5)$$

Table 3
 Enthalpies of the C–N and C–C bonds hemolytic cleavage reactions at 298 K in **1** and **2** and experimental activation energies of **1** and **2** thermal decomposition

Method	1,1-Dinitroethane		1,2-Dinitroethane	
	C–N	C–C	C–N	C–C
Experiment	49.0 [2] 47.1 [4]	91.7 [4]	62.0 [2]	—
B3LYP/6-31G(d)	39.8	90.1	53.2	81.7
B3LYP/6-311G(2df,p)	38.7	87.8	51.8	80.3
B3LYP/6-311++G(df,p)	37.1	87.3	50.6	77.8
B3LYP/6-311++G(3df,3pd)	37.2	86.9	51.1	77.7
CBS-QB3	49.3	97.7	61.3	88.9
G3B3	50.6	97.4	60.7	89.5

where E_a is the activation energy, T is the average temperature interval in which the experiment was carried out, and R is the universal gas constant.

The temperature at which pyrolysis of nitroalkanes is usually studied in the laboratory is in the range of 500 to 800 K. For our calculations we took $RT \approx 1.3$ kcal/mol ($T = 650$ K).

Although CBS-QB3 and G3B3 composite methods slightly overestimate enthalpies of C–N bond cleavage in **1**, enthalpies of C–N bond dissociation of **1** and **2** are in good agreement with experiments. The results of B3LYP level are much less accurate (Table 3). However, the enthalpies of the C–C bond cleavage obtained at B3LYP level of theory are in good agreement with experiments, whereas composite methods overestimate $\Delta H_r^0(\text{C–C})$ significantly. This coincidence between experimental and B3LYP-calculated data can be explained by the cancellation of errors in enthalpies of formations of initial compounds and radical products during the calculation of $\Delta H_r^0(\text{C–C})$ in accordance with Eq. (3). Results of Table 1 demonstrate the poor agreement between experimental enthalpies of formation of **1** and those predicted at B3LYP levels of theory. Thus, we suppose that experimental data for the activation energy of C–C bond cleavage is underestimated and can only be used for very rough estimates.

As one can see from Table 4, calculated activation enthalpies for reaction of HONO elimination from **1** and **2** using composite methods seem to be in good agreement with experimental estimations [2] (Table 4).

On the other hand, Manelis et al. [4] reported that accumulation of the nitro group had decreased the activation energies of HONO elimination in nitroalkanes. Furthermore, Denis et al. [5] showed that activation enthalpies of HONO elimination from nitroethane and 2-nitropropane at B3LYP/6-311+G(3df,2p) are 42.0 and 39.2 kcal/mol, respectively, whereas experimental activation energies for these reactions are 45.0 and 43.5 kcal/mol. The activation energies for HONO elimination from 1,1-, 1,2-, and 2,2-dinitropropane reported by Shaw [2] are 43.0, 41.0, and 39.0 kcal/mol, respectively. Thus, we assume that Shaw's experimental as well as our G3B3 and

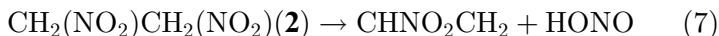
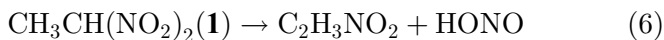
Table 4
 Activation enthalpies of the HONO elimination at 298 K from **1** and **2** and experimental activation energies

Method	Compounds	
	1,1-Dinitroethane	1,2-Dinitroethane
Experiment [2]	E_a (kcal/mol)	47.0
B3LYP/6-31G(d)	ΔH_{298}^\ddagger (kcal/mol)	42.3
B3LYP/6-311G(2df,p)		38.5
B3LYP/6-311++G(df,p)		39.0
B3LYP/6-311++G(3df,3pd)		39.2
CBS-QB3		44.9
G3B3		44.8

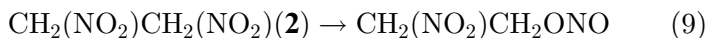
CBS-QB3 calculated values for HONO elimination from **1** and **2** are overestimated.

On the basis of comparison of calculated enthalpies of formation and activation enthalpies with available experimental data we concluded that the G3B3 model chemistry calculations do provide a reasonable way to tackle the problem of the decomposition channels of **1** and **2**.

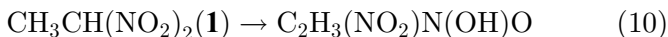
In further discussion of mechanisms of decomposition we will deal with activation enthalpies and enthalpies of reactions at 298 K. There are three main nonradical channels for **1** and **2**. The first mechanism is the β -elimination of HONO.



The second possible mechanism is the nitro–nitrite rearrangement



Finally, the third mechanism involves a hydrogen transfer and isomerization of **1** and **2** to aci-form



A schematic potential energy diagram for the unimolecular decomposition reactions associated to IRC on the ground PES (concerning **1**) is shown in Fig. 2. Relative energies of stationary points on the **1** PES were estimated on the basis of sum of electronic and thermal enthalpies [15] at 298.15 K.

The optimized geometrical parameters of transition states **1b**, **1d**, **1g** (Fig. 2) and products **1c**, **1h** involved in reactions (6), (8), and (10) are collected in Fig. 3.

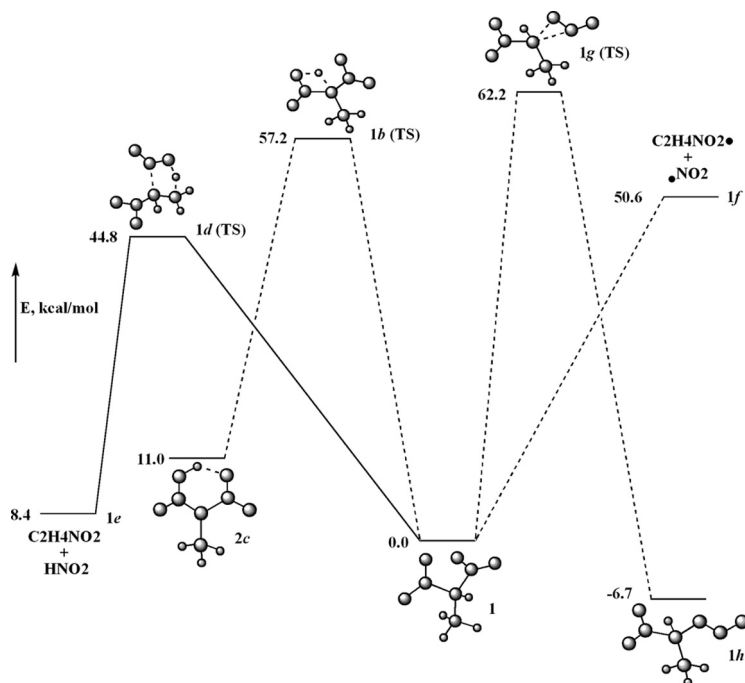


Figure 2. Schematic potential energy diagram showing the unimolecular decomposition reactions associated to IRC on the **1** ground-state PES (G3B3).

The calculated endothermicity for the C–N bond homolytic cleavage (**1** → **1f**, Fig. 3) proceeding without an apparent transition state structure using G3B3 model chemistry is 50.6 kcal/mol (Table 3, Fig. 2).

Elimination of HONO (**1** → **1d(TS)** → **1e**, Fig. 2) requires a relatively high energy to occur. This potential energy barrier is calculated to be 44.8 kcal/mol. The difference in energies of these two channels does not allow to favor any of this process, especially at the working temperature.

Regarding the transition state **1d(TS)** (Figs. 2 and 3), the planar five-centered cycle where fission of the C₃–H₆ bond is as advanced as the formation of the new H₆–O₁₂ bond. Enthalpy of the reaction **1** → **1d(TS)** → **1e** (Fig. 2) is predicted to be 11.0 kcal/mol.

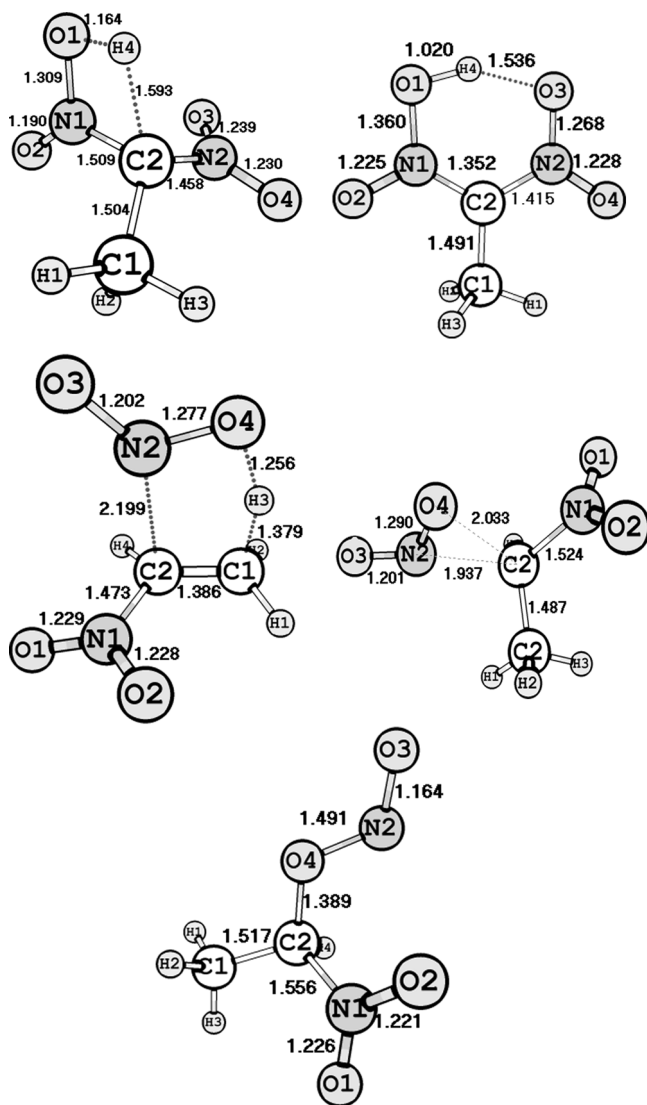


Figure 3. Geometrical parameters of transition states **1b(TS)**, **1d(TS)**, **1g(TS)**, and products **1c**, **1h** concerning the different decomposition reactions of **1** (B3LYP/6-31G(d)). Bonds distances in Å.

The next possible channel of decomposition is nitro–nitrite rearrangement (8). This reaction occurs through a pseudorotation of the NO_2 group. The resulting optimized structure, **1g(TS)** (Figs. 2 and 3), was characterized as a true transition state. At the transition state **1g(TS)** the C1–N8 bond length is 0.441 Å longer than its equilibrium value in **1** (Fig. 1). At G3B3 level of theory the energy of transition structure **1g(TS)** is calculated to be 62.2 kcal/mol. This channel seems to be the most unfavorable. In spite of the largest activation barrier height, the reaction of nitro–nitrite rearrangement is exothermic. Structure **1h** (Figs. 2 and 3) was characterized as a product of the decomposition pathway $\mathbf{1a} \rightarrow \mathbf{1g(TS)} \rightarrow \mathbf{1h}$ and is predicted to lie 6.7 kcal/mol below **1**.

The last mechanism we studied is the formation of aci-form (10) involving intramolecular migrations of the hydrogen atom. The energy of the transition state structure **1b(TS)** (Figs. 2 and 3) is predicted to be 57.2 kcal/mol. An IRC calculation starting at transition state **1b(TS)** gave a path leading to a local minimum **1c** (Figs. 2 and 3), which turned out to be an aci-form of 1,1-dinitroethane and its optimized geometry has a planar six-centered cycle C₁–N₇–O₉–H₂–O₁₁–N₈ (Fig. 3). The positive hydrogen atom (0.466 au) is located between the negatively charged oxygen atoms (–0.470 au). Charges on atoms were obtained using Mulliken population analysis. Equilibrium structure **1c** is predicted to lie 11.0 above **1** (Fig. 2).

We made several efforts to study the reaction of carbene formation proceeding through α -elimination of HONO from **1** and **2**. However, localized transition state structures were characterized as true transition states for aci-form formation. Therefore, we suppose that carbene formation takes place via elimination of HONO fragment from aci-form.

Regarding the decomposition of **2**, the HONO elimination pathway (7) seems to be the most favorable (Fig. 4). The calculated potential energy barrier for the HONO elimination ($[\mathbf{2} \rightarrow \mathbf{2b(TS)} \rightarrow \mathbf{2c}]$; Fig. 4) is 43.3 kcal/mol. The resulting optimized structure, **2b(TS)** (Fig. 5), was characterized as a true transition structure. The enthalpy of reaction is calculated to be 11.5 kcal/mol (Fig. 4).

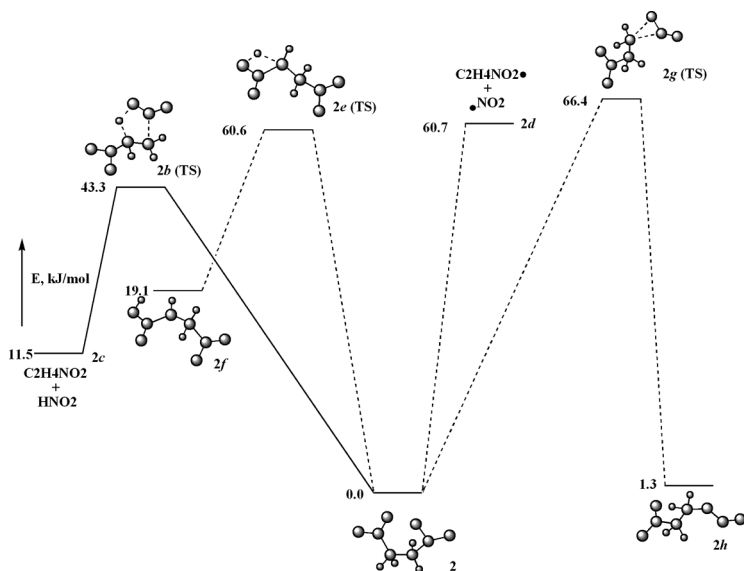


Figure 4. Schematic potential energy diagram showing the unimolecular decomposition reactions associated to IRC on the $\mathbf{2}$ ground-state PES (G3B3).

The homolytic C–N bond cleavage mechanism ($\mathbf{2} \rightarrow \mathbf{2d}$, Fig. 4) requires a higher energy barrier, than HONO elimination, energy to occur, 60.7 kJ/mol.

The optimized structure $\mathbf{2e(TS)}$ (Figs. 4 and 5) was characterized as a true transition state for reaction of aci-form formation ($\mathbf{2} \rightarrow \mathbf{2e(TS)} \rightarrow \mathbf{2f}$, Fig. 4) is calculated to lie 60.6 kcal/mol above $\mathbf{2}$ (Fig. 4). The G3B3-calculated endothermicity of this decomposition channel is 19.1 kcal/mol.

Finally, the last path, nitro–nitrite rearrangement ($\mathbf{2} \rightarrow \mathbf{2g(TS)} \rightarrow \mathbf{2h}$, Fig. 4), requires very high energy, making this channel of decomposition the most unlikely of the possible processes. Beginning IRC calculations at transition state $\mathbf{2h(TS)}$ (Fig. 5), a path leading to the equilibrium structure $\mathbf{2g}$ (1-nitro,1-nitrite ethane) (Fig. 5) is calculated to lie 1.3 kcal/mol above $\mathbf{2}$.

The activation enthalpies of nitro–nitrite rearrangement and aci-form formation are significantly higher than activation enthalpies of HONO elimination and homolytic C–N bond cleavage. Therefore, we decided not to take in consideration reactions of carbene formation from aci-form and NO• loss from nitrite isomers of **1** and **2**.

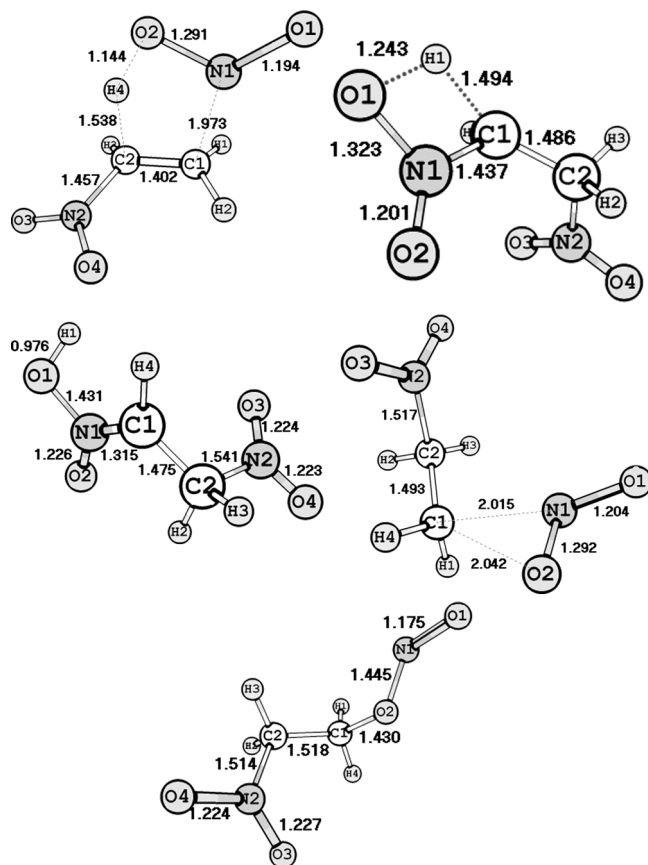


Figure 5. Geometrical parameters of transition states **2b(TS)**, **2e(TS)**, **2g(TS)**, and products **2f**, **2h** concerning the different decomposition reactions of **2** (B3LYP/6-31G(d)). Bond distances in Å.

Conclusion

The gas-phase enthalpies of formation of 1,1- and 1,2-dinitroethane and corresponding radical products were calculated using G3B3, CBS-QB3 composite methods and DFT B3LYP level of theory with various basis sets. The enthalpies of the C–N, C–C bonds' dissociation and activation enthalpies for HONO elimination were also calculated and compared with available experimental data. In the cases of enthalpies of formation and of the potential energy surfaces themselves, the scarce experimental data available seem to agree well with our calculations. Therefore, we conclude that the G3B3 calculations do provide a reasonable way to tackle the problem of the decomposition channels of dinitroalkanes.

We have performed a study of important decomposition channels on the potential energy surface of 1,1- and 1,2-dinitroethane. HONO elimination seems to be the most favorable mechanism for the decomposition of 1,2-dinitroethane, whereas the difference in energies of the HONO elimination and C–N homolytic bond cleavage in 1,1-dinitroethane does not allow to favor any of these channels, especially at the working temperature. The nitro–nitrite rearrangement that occurs through a pseudorotation of the NO_2 group is the most unlikely of the possible processes.

Gauche-conformation of 1,2-dinitroethane is calculated to be the lowest energy minimum on the potential energy surface at various levels of theory.

Acknowledgment

Our calculations were realized using the Interdepartmental Supercomputer Center (Moscow).

References

- [1] Spokes, G. N. and S. W. Benson. 1967. Very low pressure pyrolysis. II. Decomposition of nitropropanes. *Journal of the American Chemical Society*, 89: 6030–6035.

- [2] Shaw, R. 1973. Heats of formation and kinetics of decomposition of nitroalkanes. *International Journal of Chemical Kinetics*, 5: 261.
- [3] Wodtke, A. M., E. J. Hints, and Y. T. Lee. 1986. Infrared multiphoton dissociation of three nitroalkanes. *Journal of Physical Chemistry*, 90: 3549–3558.
- [4] Manelis, G. B., G. M. Nazin, Yu. I. Rubtsov, and V. A. Strunin. 2003. *Thermal Decomposition and Combustion of Explosives and Propellants*. London: Taylor & Francis.
- [5] Denis, P. A., O. N. Ventura, H. T. Le, and M. T. Ngyen. 2003. Density functional study of the decomposition pathways of nitroethane and 2-nitropropane. *Physical Chemistry Chemical Physics*, 5: 1730–1738.
- [6] Hohenberg, P. and W. Kohn. 1964. Inhomogeneous electron gas. *Physical Review*, 136: 854.
- [7] Kohn, W. and L. J. Sham. 1965. Self-consistent equations including exchange and correlation effects. *Physical Review*, 140: 1133.
- [8] Becke, A. D. 1993. Density functional thermochemistry. III. The role of exact exchange. *Journal of Chemical Physics*, 98: 5648–5652.
- [9] Lee, C., W. Yang, and R. G. Parr. 1988. Development of the Colle-Salvetti correlation-energy formula into a functional of the electron density. *Physical Review B*, 37: 785–789.
- [10] Miehlich, B., A. Savin, H. Stoll, and H. Preuss. 1989. Results obtained with the correlation energy density functionals. *Chemical Physics Letters*, 157: 200–206.
- [11] Hehre, W. J., L. Radom, P. V. Schleyer, and J. Pople. 1986. *Ab Initio Molecular Orbital Theory*. Wiley.
- [12] Baboul, A. G., L. A. Curtiss, P. C. Redfern, and K. Raghavachari. 1999. Gaussian-3 theory using density functional geometries and zero-point energies. *Journal of Chemical Physics*, 110: 7650–7657.
- [13] Montgomery, J. A. Jr., M. J. Frisch, J. W. Ochterski, and G. A. Petersson. 1999. A complete basis set model chemistry. VI. Use of density functional geometries and frequencies. *Journal of Chemical Physics*, 110: 2822–2827.
- [14] Montgomery, J. A. Jr., M. J. Frisch, J. W. Ochterski, and G. A. Petersson. 2000. A complete basis set model chemistry. VII. Use of the minimum population localization method. *Journal of Chemical Physics*, 112: 6532–6542.

- [15] Frisch, M. J., G. W. Trucks, H. B. Schlegel, G. E. Scuseria, M. A. Robb, J. R. Cheeseman, J. A. Montgomery, Jr. T. Vreven, K. N. Kudin, J. C. Burant, J. M. Millam, S. S. Iyengar, J. Tomasi, V. Barone, B. Mennucci, M. Cossi, G. Scalmani, N. Rega, G. A. Petersson, H. Nakatsuji, M. Hada, M. Ehara, K. Toyota, R. Fukuda, J. Hasegawa, M. Ishida, T. Nakajima, Y. Honda, O. Kitao, H. Nakai, M. Klene, X. Li, J. E. Knox, H. P. Hratchian, J. B. Cross, C. Adamo, J. Jaramillo, R. Gomperts, R. E. Stratmann, O. Yazyev, A. J. Austin, R. Cammi, C. Pomelli, J. W. Ochterski, P. Y. Ayala, K. Morokuma, G. A. Voth, P. Salvador, J. J. Dannenberg, V. G. Zakrzewski, S. Dapprich, A. D. Daniels, M. C. Strain, O. Farkas, D. K. Malick, A. D. Rabuck, K. Raghavachari, J. B. Foresman, J. V. Ortiz, Q. Cui, A. G. Baboul, S. Clifford, J. Cioslowski, B. B. Stefanov, G. Liu, A. Liashenko, P. Piskorz, I. Komaromi, R. L. Martin, D. J. Fox, T. Keith, M. A. Al-Laham, C. Y. Peng, A. Nanayakkara, M. Challacombe, P. M. W. Gill, B. Johnson, W. Chen, M. W. Wong, C. Gonzalez, and J. A. Pople. 2003. *Gaussian 03*, Rev. B. 04. Pittsburgh, PA: Gaussian, Inc.
- [16] Tafipolsky, M. A., I. V. Tokmakov, and V. A. Shlyapochnikov. 1999. Structure and vibrational spectra of dinitromethane and trinitromethane. *Journal of Molecular Structure*, 510: 149–156.
- [17] Kiselev, V. G. and N. P. Gritsan. 2008. Theoretical study of the nitroalkane thermolysis. 1. Computation of the formation enthalpy of the nitroalkanes, their isomers and radical products. *Journal of Physical Chemistry*, 112: 4458–4464.
- [18] Lam, Y.-L., L. L. Koh, and H. H. Huang. 1993. IR spectra, crystal structure, dipole moment, ab-initio and AM1 study of 1,2-dinitroethane. *Journal of the Chemical Society Perkin Transactions*, 2: 175–180.
- [19] Lebedev, Y. A., E. A. Miroshnichenko, and Y. K. Knobel. 1970. *Thermochemistry of Nitrocompounds*. Moscow: Nauka. (in Russian)
- [20] Gurvich, L. V., I. V. Veyts, and C. B. Alcock. Thermodynamic properties of individual substances. In P. J. Linstrom and W. G. Mallard (eds.), *NIST Chemistry WebBook*, NIST Standard Reference Database 69. Gaithersburg, MD: NIST. Available at: <http://webbook.nist.gov/Chemistry> [accessed September 1, 2010]
- [21] Redfern, P. C., P. Z. Larry, A. Curtiss, and K. Raghavachari. 2000. Assessment of Gaussian-3 and density functional theories for enthalpies of formation of C₁–C₁₆ alkanes. *Journal of Physical Chemistry A*, 104: 5850–5854.